

Supporting Information

Negative Poisson's ratio of sulfides dominated by strong intralayer electron repulsion
~~Negative Poisson's ratio in transition metal dichalcogenides dominated by strong intra-layer electronic interaction~~

Yucheng Zhu¹, Xiaofei Cao¹, Shuaijun Yang¹, Jun Hu^{1,*}, Baotong Li^{2,*}, Zhong Chen^{3,*}

¹ School of Chemical Engineering, Northwest University, Xi'an, 710069 P. R. China;

² Key Laboratory of Education Ministry for Modern Design & Rotor-Bearing System, Xi'an Jiaotong University, Xi'an, 710049, P.R. China;

³ School of Materials Science and Engineering, Nanyang Technological University, 50 Nanyang Avenue, 639798 Singapore

*Corresponding Authors: E-mail: hujun32456@163.com (JH); ASZChen@ntu.edu.sg (ZC); baotong.me@xjtu.edu.cn (BL)

Table S1 Calculated lattice parameters for a, b, and c (in Å), α , β , and γ (in degrees) for chalcopyrite-structured sulfide-type LiMS_2 (M = Sc, Ti, V, Cr, Mn, Fe, Co, and Ni).

	<u>a</u>	<u>b</u>	<u>c</u>	<u>α</u>	<u>β</u>	<u>γ</u>
<u>LiScS_2 (this work)</u>	<u>5.78</u>	<u>5.78</u>	<u>10.94</u>	<u>90</u>	<u>90</u>	<u>90</u>
<u>LiScS_2 (ref.1)</u>	<u>5.72</u>	<u>5.72</u>	<u>11.35</u>	<u>90</u>	<u>90</u>	<u>90</u>
<u>LiTiS_2 (this work)</u>	<u>5.73</u>	<u>5.73</u>	<u>10.77</u>	<u>90</u>	<u>90</u>	<u>90</u>
<u>LiTiS_2 (ref.1)</u>	<u>5.65</u>	<u>5.65</u>	<u>10.80</u>	<u>90</u>	<u>90</u>	<u>90</u>
<u>LiVS_2 (this work)</u>	<u>5.48</u>	<u>5.48</u>	<u>10.77</u>	<u>90</u>	<u>90</u>	<u>90</u>
<u>LiVS_2 (ref.1)</u>	<u>5.56</u>	<u>5.56</u>	<u>10.72</u>	<u>90</u>	<u>90</u>	<u>90</u>
<u>LiCrS_2 (this work)</u>	<u>5.65</u>	<u>5.65</u>	<u>10.07</u>	<u>90</u>	<u>90</u>	<u>90</u>
<u>LiCrS_2 (ref.1)</u>	<u>5.68</u>	<u>5.68</u>	<u>10.05</u>	<u>90</u>	<u>90</u>	<u>90</u>
<u>LiMnS_2 (this work)</u>	<u>5.45</u>	<u>5.45</u>	<u>10.77</u>	<u>90</u>	<u>90</u>	<u>90</u>
<u>LiMnS_2 (ref.1)</u>	<u>5.54</u>	<u>5.54</u>	<u>10.71</u>	<u>90</u>	<u>90</u>	<u>90</u>
<u>LiFeS_2 (this work)</u>	<u>5.39</u>	<u>5.39</u>	<u>9.77</u>	<u>90</u>	<u>90</u>	<u>90</u>
<u>LiFeS_2 (ref.1)</u>	<u>5.49</u>	<u>5.49</u>	<u>9.72</u>	<u>90</u>	<u>90</u>	<u>90</u>
<u>LiCoS_2 (this work)</u>	<u>5.40</u>	<u>5.40</u>	<u>9.77</u>	<u>90</u>	<u>90</u>	<u>90</u>
<u>LiCoS_2 (ref.1)</u>	<u>5.48</u>	<u>5.48</u>	<u>9.78</u>	<u>90</u>	<u>90</u>	<u>90</u>
<u>LiNiS_2 (this work)</u>	<u>5.38</u>	<u>5.38</u>	<u>10.67</u>	<u>90</u>	<u>90</u>	<u>90</u>
<u>LiNiS_2 (ref.1)</u>	<u>5.41</u>	<u>5.41</u>	<u>10.19</u>	<u>90</u>	<u>90</u>	<u>90</u>

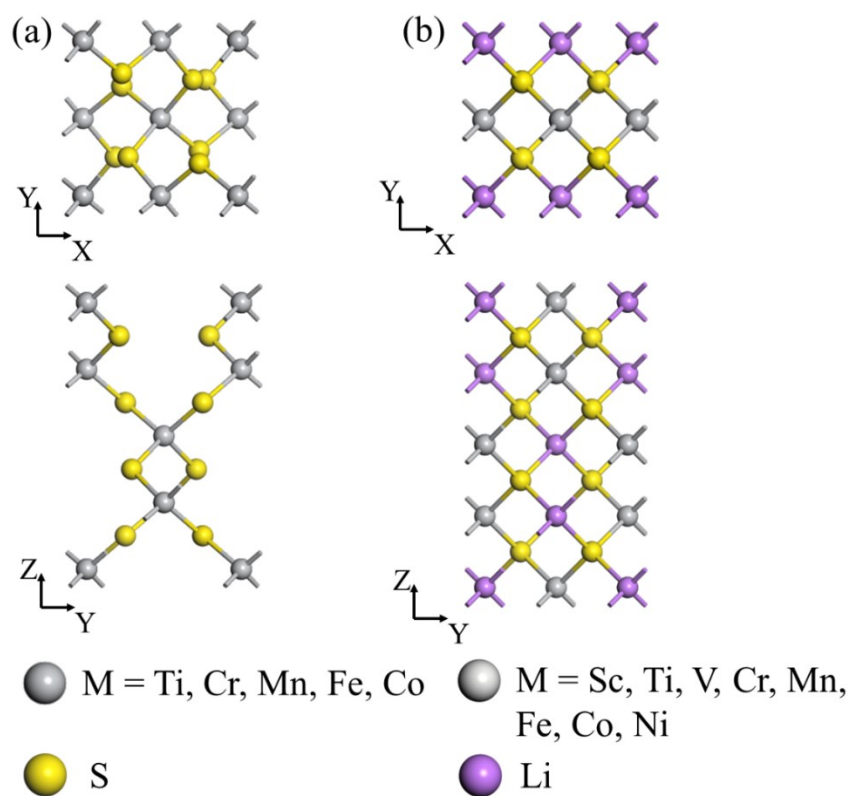


Fig. S1 The views of the geometry structures of MS_2 ($M = \text{Ti, Cr, Mn, Fe, Co}$) and chalcopyrite-structured sulfide-type $LiMS_2$ ($M = \text{Sc, Ti, V, Cr, Mn, Fe, Co, Ni}$).

Supplementary Note 1

The dynamic and thermal stability of MS_2 compounds were evaluated through phonon calculations and MD simulations. The phonon branches in Fig. S2 indicate that these monolayer MS_2 compounds are dynamically stable, as there are no imaginary frequencies present. Additionally, MD simulations were conducted to assess the thermal stability. The results are presented in Fig. S2. During the simulation, the atomic potential energy stays consistent and hovers around the average value. The temperature profiles at 300 K and the structural snapshots after MD simulation suggest that the geometry is well conserved, and no structural fractures are observed. This suggests that the monolayer MS_2 exhibits favorable thermal stability at high temperatures.

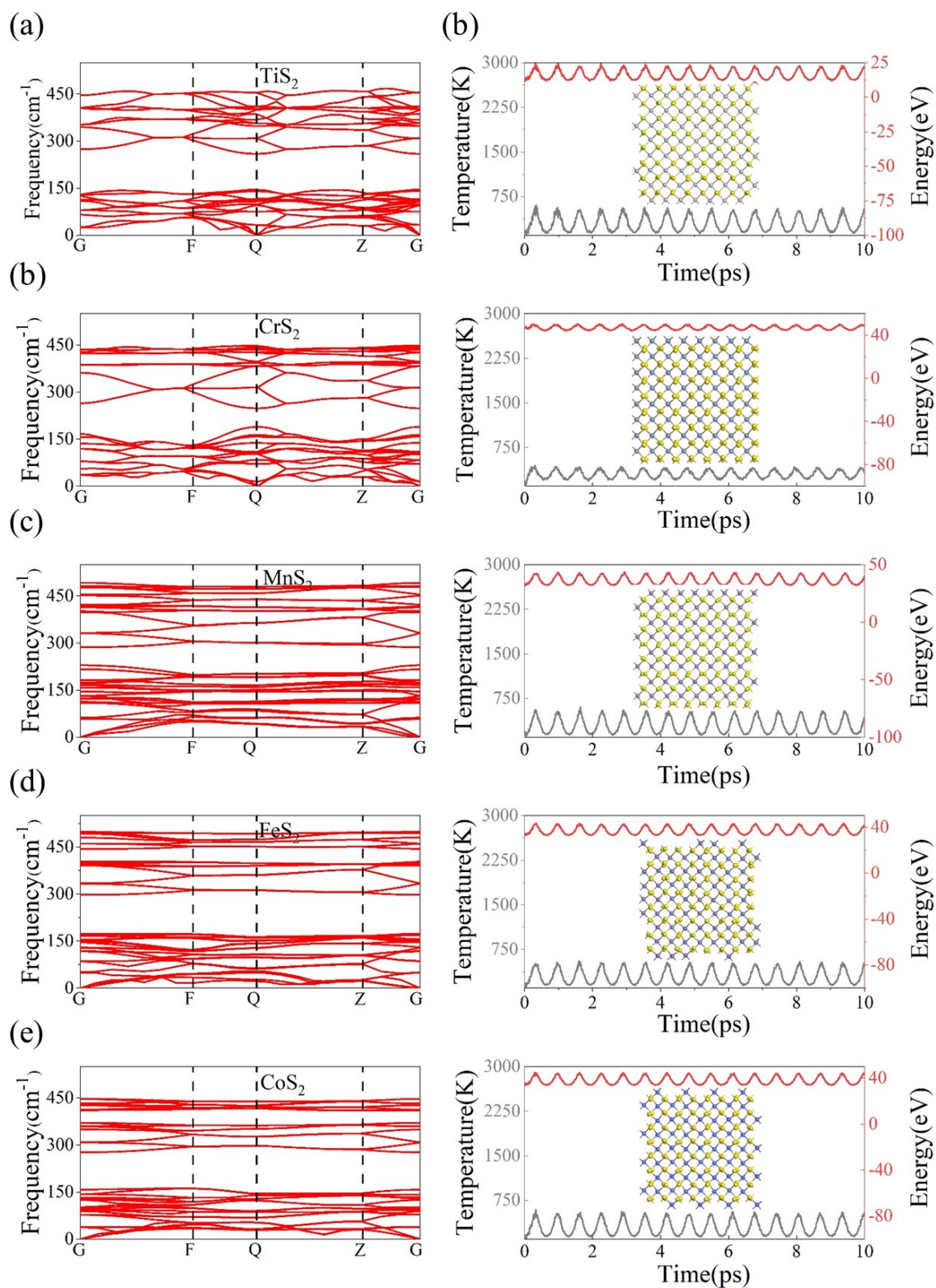


Fig. S1-S2 Phonon spectra (left) and molecular dynamics simulations at 300 K (right) for (a) TiS_2 , (b) CrS_2 , (c) MnS_2 , (d) FeS_2 , and (e) CoS_2 ; temperature fluctuations (gray line), total energy fluctuations (red line), and snapshots after 10 ps).

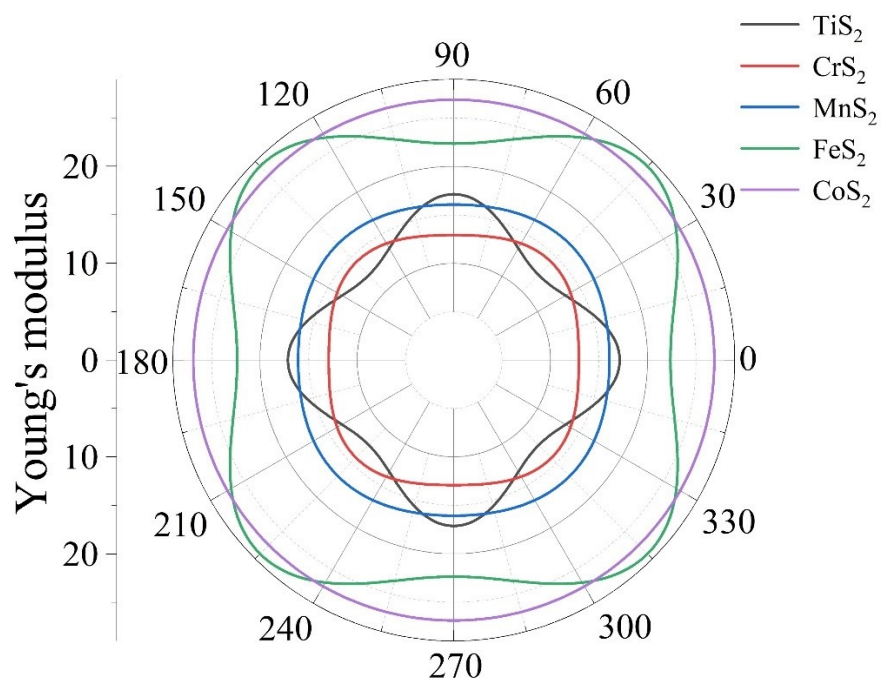


Fig. S2-S3 Young's modulus of monolayer MS_2 as a function of the angle θ . $\theta = 0^\circ$ corresponds to the X-axis.

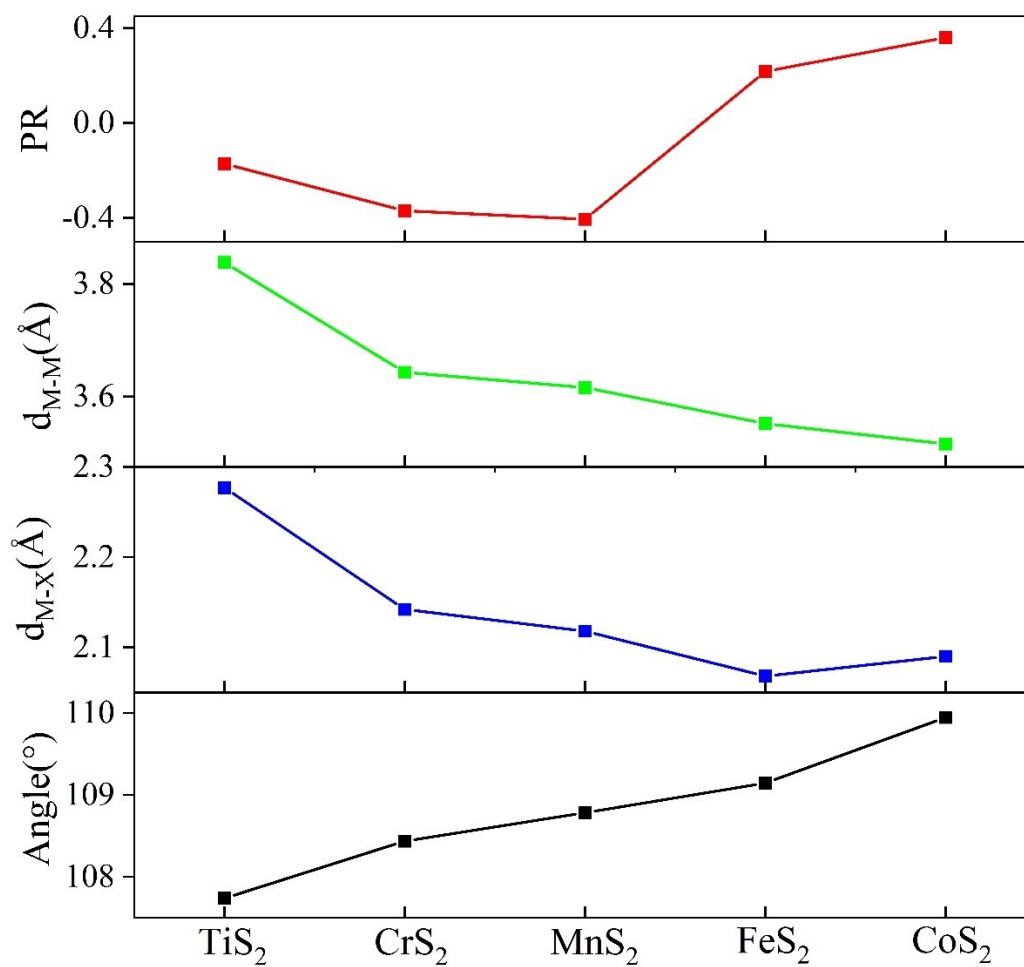


Fig. S3-S4 The Poisson's ratio of the MS₂ compounds under strain along the X-direction is shown along with other geometrical parameters, including the M-M spacing (d_{M-M}), the M-S-M angle along the longitudinal direction ($\angle MSM$) and the M-S spacing (d_{M-X}).

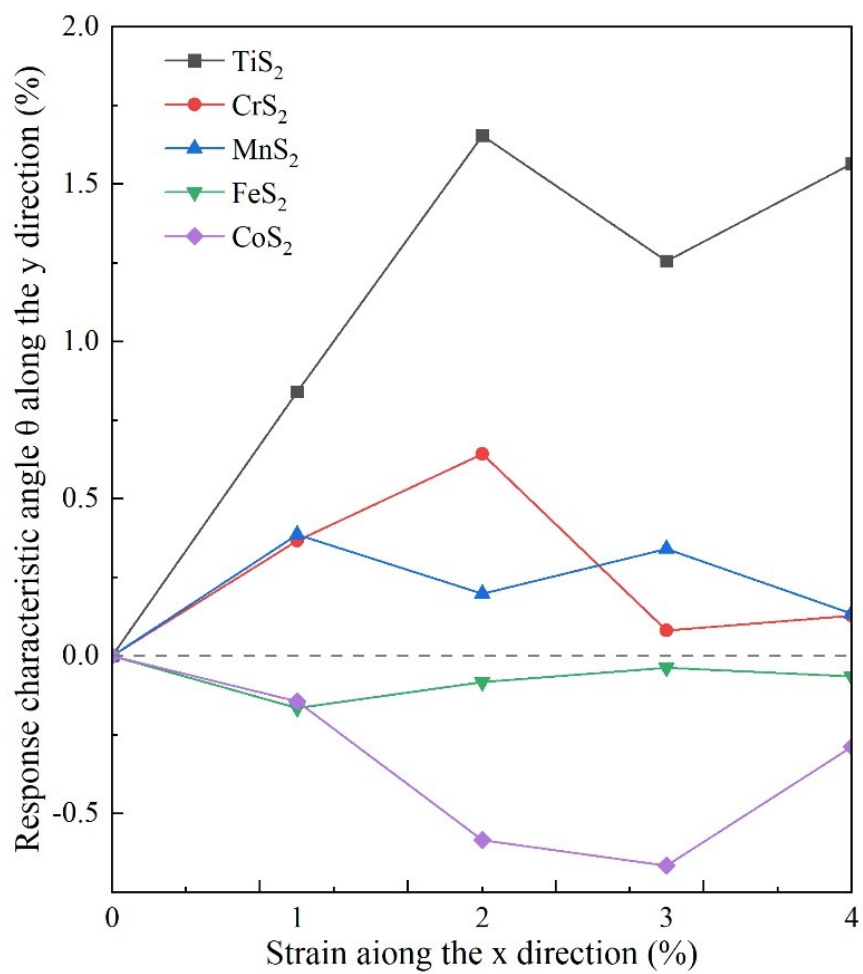


Fig.S5 MS_2 Strain-driven characteristic angles θ response along the x-direction.

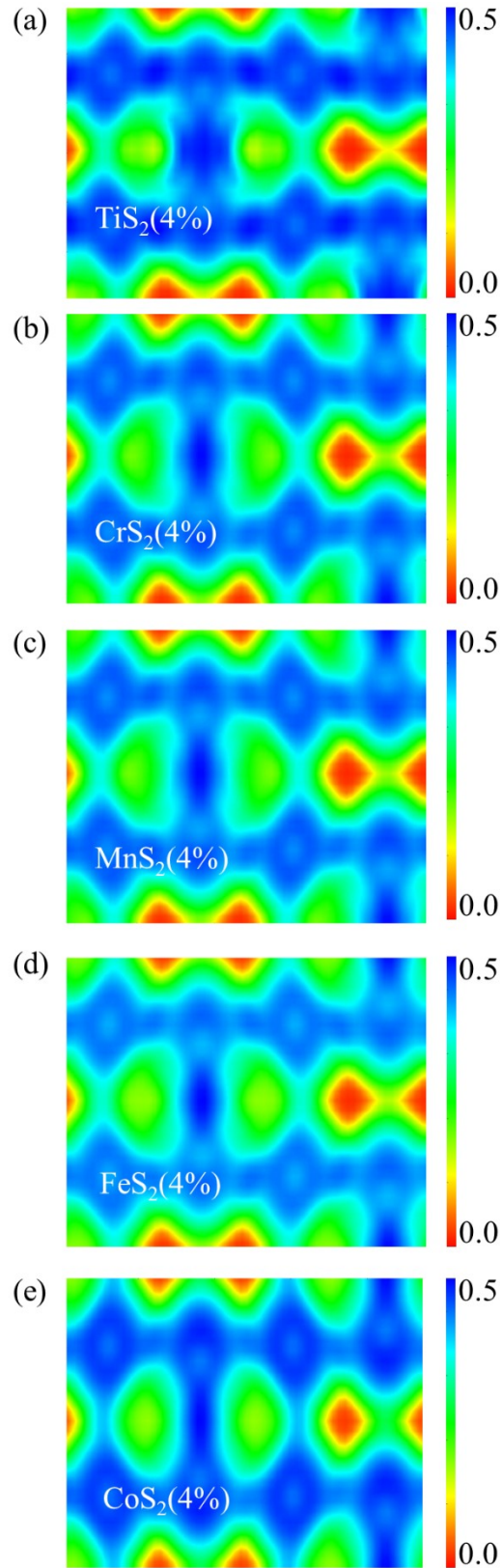


Fig. S4-S6 (a) ELF of TiS_2 at 4% strain. (b) ELF of CrS_2 at 4% strain. (c) ELF of MnS_2 at 4% strain. (d) ELF of FeS_2 at 4% strain. (e) ELF of CoS_2 at 4% strain.

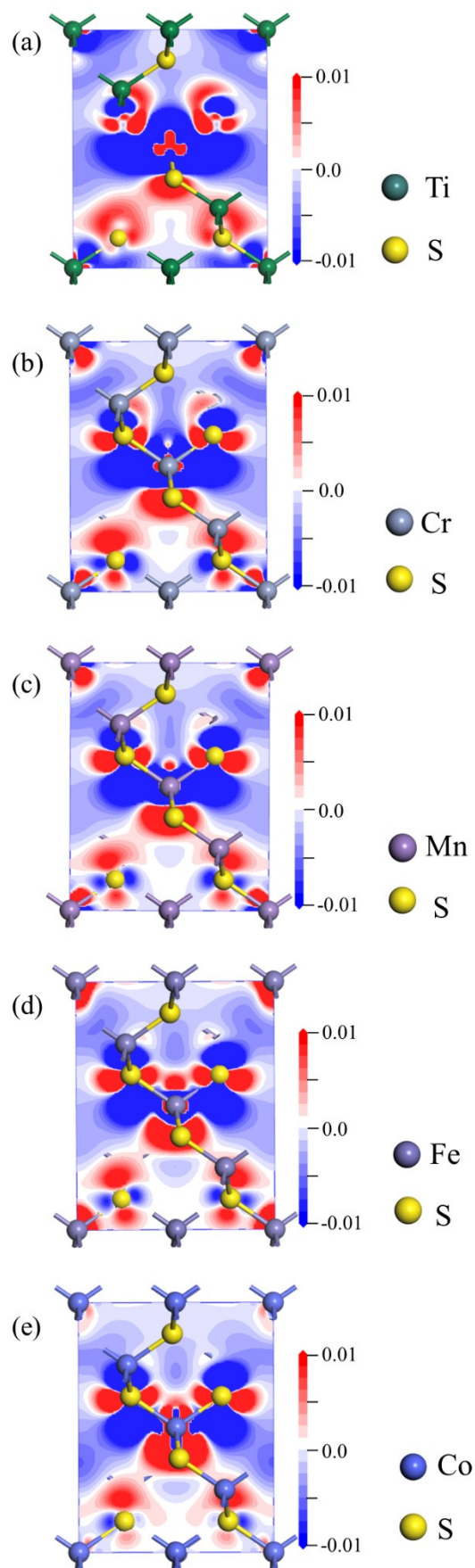


Fig. S7 Electron density difference map of (a) TiS_2 , (b) CrS_2 , (c) MnS_2 , (d) FeS_2 and (e) CoS_2 . In

an electron density difference map, the loss of electrons is indicated by a blue coloration, while the gain of electrons is indicated by a red coloration. The white color indicates regions where there is minimal variation in electron density.

Supplementary References

1 Z. Xu, S. Bo, H. Zhu, LiCrS_2 and LiMnS_2 Cathodes with Extraordinary Mixed Electron–Ion Conductivities and Favorable Interfacial Compatibilities with Sulfide Electrolyte, *ACS Appl. Mater. Interfaces* 2018, 10, 36941–36953.